SUPPLEMENTARY METHODS

Animals and procedures

All animal experiments were approved by IACUC and carried out in accordance with institutional guidelines. Adult (age 10–12 weeks) C57BL/6 mice were purchased from Jackson Laboratories (Bar Harbor, ME, USA), maintained in a temperature- and light-controlled facility, and permitted ad libitum consumption of water and standard pellet chow. Warfarin (1 µg/mL) was administered to mice by adding the drug to drinking water as previously described [1]. This dose in pilot studies achieved a doubling of international normalized ratio (INR) from baseline. INR levels were measured from blood obtained after tail snip using CoaguChek® XS System (Roche).

Bile duct ligation

Mice were subjected to bile duct ligation (BDL) or SHAM operation for 2 weeks to induce fibrosis as described [2].

Portal pressure measurements

Portal pressure was directly measured using a digital blood pressure analyzer (Digi-Med) with a computer interface [3]. Once the analyzer was calibrated, a 16-gauge catheter attached to the pressure transducer was inserted into the portal vein and sutured in place. The pressure was continuously monitored, and the average portal pressure was recorded. Prior to sacrifice, the suprahepatic IVC was transected and the liver was perfused with 10 mL of 1X PBS through the portal vein to remove circulating fibrinogen [4]. The spleen and liver were harvested, weighed and spleen/body and liver/body weight ratios were calculated. Liver aliquots were snap frozen in

liquid nitrogen for Western blotting, mRNA extraction and hydroxyproline, Tissue-Tek (Sakura Finetek) fixation for frozen sectioning, or fixed in 10% formaldehyde for histology.

2D-Echocardiogram

Echocardiogram was performed 6 weeks after pIVCL or SHAM, as previously described [5]. Left ventricular internal diameter in diastole (LVIDd) and in systole (LVIDs), fractional shortening (FS), ejection fraction and left ventricular mass were obtained. LV end diastolic and systolic volumes, stroke volume and cardiac output were calculated as described [5].

Serum analyses and LPS-BP Elisa

Serum was collected from whole blood of each animal at time of sacrifice and transferred into 3.5 ml serum separating tubes. Specimens were processed and analyzed for serum transaminases and total and indirect bilirubin by the Animal Clinical Chemistry Core Facility at University of North Carolina. Serum levels of LPS binding protein (LPSBP) were determined using a sandwich ELISA (Abnova Corporation), as recommended by the manufacturer instructions.

Cell culture and isolation

Primary murine (mHSC) or human HSC (hHSC; ScienCell Research Laboratories) [6, 7] were used in these studies as indicated in individual figure legends. Cells were cultured in Dulbecco's Modified Eagle's Medium supplemented with 10% FBS, 1 mmol/L l-glutamine, and 100 IU/mL streptomycin/penicillin. Plastic-ware was thin-coated with 1 mg/ml bovine fibrinogen, 1 mg/ml fibrinogen plus 0.2 U/ml thrombin to form fibrin, or 1 mg/ml collagen IV as control, overnight at 4°C. The dishes were then washed with PBS and blocked with 0.1% BSA for 30 min at 37 °C. Serum-starved hHSC were seeded on coated dishes in basal DMEM for the indicated time before protein or mRNA extraction.

Mechanical cyclic stretch

Primary human and murine HSC were seeded on 6-well plates of flexible silicone bottom coated with collagen type IV (FLEX I® culture plates) at 0.3 $X10^6$ cells/well. After incubation for 24 hours, cells were serum-starved overnight and then subjected to cyclic uniform stretch for 6-24 hours, as previously described [8]. Oscillatory displacement with strain amplitude of 10% was used at a rate of 30 cycles/min at 37 °C and 5% CO2 in a humidified incubator. These strain conditions were based on physiologically relevant strain values as per Sakata et al [9].

Fibrin gels

Fibrin gels were constructed as described with or without cells seeded within the gel [7]. hHSCs were cultured on the gels for 5 days and treated with vehicle, rat anti-human integrin antibody (MabB13; 1:200) or cytochalasin D (1:1000).

Western blot

HSC or liver tissue were lysed and prepared for Western blot analysis as previously described [2]. HSC supernatant was also collected and protein concentration was normalized by cell lysates. Immunoblot was performed according to the protocol recommended for individual antibodies, α-SMA (Sigma), FN (Santa Cruz), fibrin(ogen) (Molecular Innovations), GAPDH (Ambion) and β actin (Sigma). Immunoreactive bands were visualized using horseradish peroxidase-conjugated secondary antibody and the
enhanced chemiluminescent system (Santa Cruz Biotechnology, Inc.). All experiments were done in triplicates and quantitation was done by densitometry.

Quantitative Real-Time Polymerase Chain Reaction

Real-time fluorescence monitoring was performed with the Applied Biosystems 7500 Real Time PCR System instrument as described previously [10]. *TIMP1*, *pro-collagen1 α1, α-SMA* and *FN* mRNA were normalized to *Gapdh* or *β-actin* mRNA, with results shown as fold change. Primer sequences are listed in Supplementary Table 3.

Hydroxyproline assay

Hydroxyproline content in whole liver specimens was quantified colorimetrically as described [11]. Hydroxyproline concentration was calculated from a standard curve prepared with high-purity hydroxyproline (Sigma) and expressed as µg/mg liver tissue.

Immunohistochemistry, Immunofluorescence and morphometry

Embedded liver blocks were sectioned (5-µm) and fixed in ice-cold acetone or methanol for 15 min. Samples were blocked with 10% goat serum in PBS for 1 hour and then incubated with mouse anti-SMA (Sigma, 1:1000), mouse anti-FN (BD,1:500) or rabbit anti-fibrin(ogen) (Molecular Innovations, 1:1000) overnight at 4°C, followed by incubation for 1 hour with Alexa Fluor 546-conjugated goat anti-mouse (1:250) and Alexa Fluor 488-conjugated goat anti-rabbit (1:250) secondary antibodies. The slides were then counterstained with TOTO3, and confocal microscopy was performed by LSM 5 Pascal (Zeiss), in which appropriate laser and filter combinations were selected according to excitation and emission spectrum features of the Alexa fluorochromes.

MetaView software was used for quantification of staining intensity (Universal Imaging, Downingtown, PA) as described [7]. For morphometry, livers were fixed in 10% phosphate-buffered formalin for 48 h at 4°C, washed twice with water, stored in 70% ethanol at 4°C, and embedded in paraffin. After deparaffinization and hydration, sections (5 µM) were stained with picro-sirius red (Sigma) and counterstained with fast green (Sigma). Sirius red was quantitated in randomly chosen sections (×20; 10 fields each from sample) with MetaView software as

described [7]. For cell microscopy, biotinylated FN was added to hHSC and cells were stretched for 6 hours as described above. Cells were washed, fixed with 4% paraformaldehyde solution for 10 minutes at room temperature and then incubated with FITC labeled streptavidin (BD, 1:1000) for 1 hour. Fluorescence was visualized with Zeiss LSM 5 Pascal, and images were processed with LSM image software.

Statistical analysis

Results are expressed as means ± SE. Significance was established using the Student's t-test and analysis of variance when appropriate. Differences were considered significant when $P < 0.05$.

REFERENCES

1. Anstee QM, Goldin RD, Wright M, Martinelli A, Cox R, Thursz MR. Coagulation status modulates murine hepatic fibrogenesis: implications for the development of novel therapies. Journal of thrombosis and haemostasis : JTH 2008;6:1336-43.
2. Zou L, Cao S, Kang N, Huebert RC, Shah VH. Fibronectin induces endothelial cell migration through beta1 integrin and Src-dependent phosphorylation of fibroblast growth factor receptor-1 at tyrosines 653/654 and 766. The Journal of biological chemistry 2012;287:7190-202.
3. Semela D, Das A, Langer D, Kang N, Leof E, Shah V. Platelet-derived growth factor signaling through ephrin-b2 regulates hepatic vascular structure and function. Gastroenterology 2008;135:671-9.
4. Iannacone M, Sitia G, Isogawa M, Marchese P, Castro MG, Lowenstein PR, Chisari FV, Ruggeri ZM, Guidotti LG. Platelets mediate cytotoxic T lymphocyte-induced liver damage. Nature medicine 2005;11:1167-9.
5. Franchi F, Knudsen BE, Oehler E, Textor SC, Lerman LO, Grande JP, Rodriguez-Porcel M. Non-invasive assessment of cardiac function in a mouse model of renovascular hypertension. Hypertension research : official journal of the Japanese Society of Hypertension 2013;36:770-5.
6. Cao S, Yaqoob U, Das A, Shergill U, Jagavelu K, Huebert RC, Routray C, Abdelmoneim S, Vasdev M, Leof E, Charlton M, Watts RJ, Mukhopadhyay D, Shah VH. Neuropilin-1 promotes cirrhosis of the rodent and human liver by enhancing PDGF/TGF-beta signaling in hepatic stellate cells. The Journal of clinical investigation 2010;120:2379-94.

7. Yaqoob U, Cao S, Shergill U, Jagavelu K, Geng Z, Yin M, de Assuncao TM, Cao Y, Szabolcs A, Thorgeirsson S, Schwartz M, Yang JD, Ehman R, Roberts L, Mukhopadhyay D, Shah VH. Neuropilin-1 stimulates tumor growth by increasing fibronectin fibril assembly in the tumor microenvironment. Cancer research 2012;72:4047-59.
8. Stroetz RW, Vlahakis NE, Walters BJ, Schroeder MA, Hubmayr RD. Validation of a new live cell strain system: characterization of plasma membrane stress failure. Journal of applied physiology 2001;90:2361-70.
9. Sakata R, Ueno T, Nakamura T, Ueno H, Sata M. Mechanical stretch induces TGF-beta synthesis in hepatic stellate cells. European journal of clinical investigation 2004;34:129-36.
10. Das A, Fernandez-Zapico ME, Cao S, Yao J, Fiorucci S, Hebbel RP, Urrutia R, Shah VH. Disruption of an SP2/KLF6 repression complex by SHP is required for farnesoid X receptor-induced endothelial cell migration. The Journal of biological chemistry 2006;281:39105-13.
11. Yang L, Chan CC, Kwon OS, Liu S, McGhee J, Stimpson SA, Chen LZ, Harrington WW, Symonds WT, Rockey DC. Regulation of peroxisome proliferator-activated receptor-gamma in liver fibrosis. American journal of physiology. Gastrointestinal and liver physiology 2006;291:G902-11.

SUPPLEMENTARY FIGURE AND TABLE LEGENDS

Supplement Figure 1.

The suprahepatic inferior vena cava (IVC) was circumferentially isolated (A) and a sterile flexible wire was placed on the anterior surface of the IVC (B). A 6.0 silk thread was then tightly tied around both the IVC and the wire (C). The wire was then removed and the IVC assumed the known diameter of the wire (D).

Supplement Figure 2.

Transthoracic 2-D echocardiogram was performed 6 weeks after pIVCL or SHAM. Heart rate was significantly increased after pIVCL compared to SHAM and no difference was found in ejection fraction, left ventricle mass or cardiac output between the two groups. Data represent mean ± STDEV; n=4-5, *p<0.05.

Supplement Figure 3.

Quantitative RT-PCR from whole liver mRNA was performed to evaluate the expression of proinflammatory cytokines, IL-6, TNF-α and IL-1β, 6 weeks after SHAM and pIVCL and 2 weeks after BDL surgeries. Data represent mean ± STDEV; n=8-9, *p<0.05.

Supplement Figure 4.

Serum hepatic transaminases, alanine aminotransferase (ALT) and aspartate aminotransferase (AST), and total and indirect bilirubin were unchanged after pIVCL (A). ELISA for serum lipopolysaccharide-binding protein (LBP), a surrogate for innate immunity activation, was not significantly changed after pIVCL (B). Data represent mean ± STDEV; n=8-9.

Supplement Figure 5.

Hematoxylin-Eosin stain (100X) revealed vascular congestion and minimal inflammatory infiltrates in liver after pIVCL, in contrast with marked hepatic inflammatory cell infiltration after BDL.

Supplement Figure 6.

Thrombin (10 U) was added to serum-starved hHSC. Cells were collected after six hours for mRNA extraction. qRT-PCR was performed for pro-collagen1α1, α-SMA, TIMP1 and fibronectin expression. Experiments were performed 3 times with similar results. Data represent mean ± STDEV; *$p<0.05$.

Supplement Figure 7.

Serum starved hHSC were seeded on collagen- or fibrin-coated dishes for six hours. mRNA expression of pro-collagen1α1, α-SMA and fibronectin by qRT-PCR did not differ between the two groups. . Experiments were performed 3 times with similar results. Data represent mean ± STDEV.

Supplement Table 1. Demographics of 14 patients with congestive heart failure.

Supplement Table 2. Demographics of 12 patients who had undergone corrective surgery (Fontan procedure) for complex congenital heart disease.

Supplement Table 3. Primers sequence.

Supplement Figure 1

A.

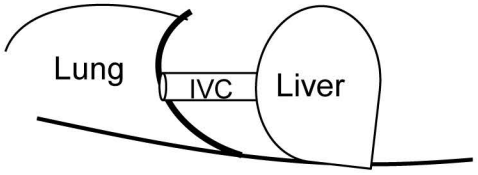

B.

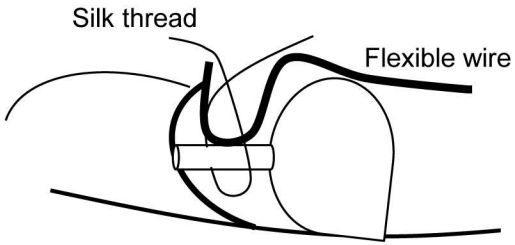

C.

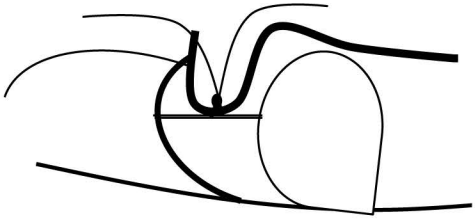

D.

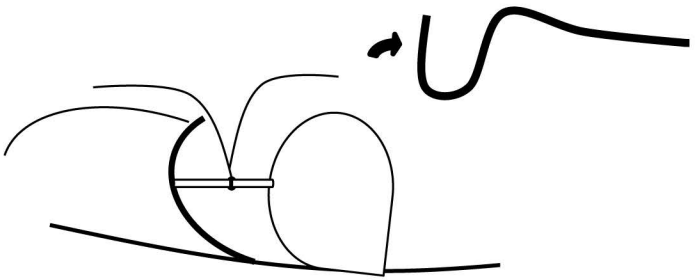

Supplement Figure 2

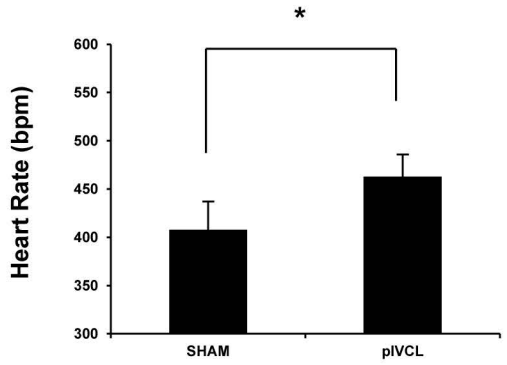

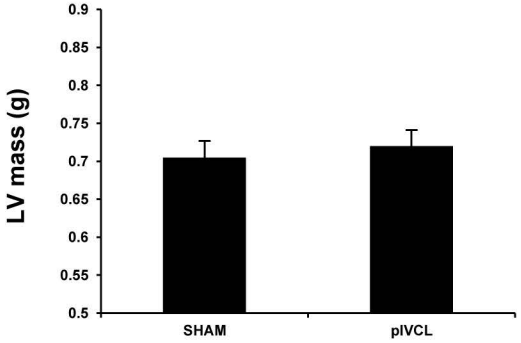

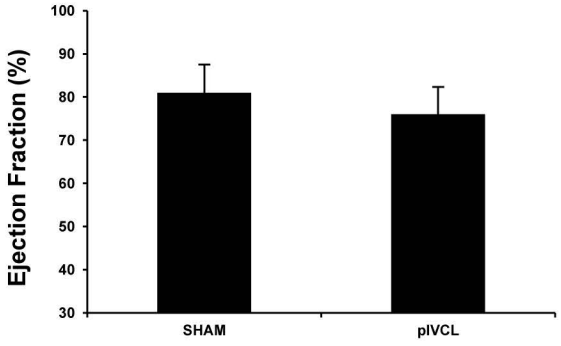

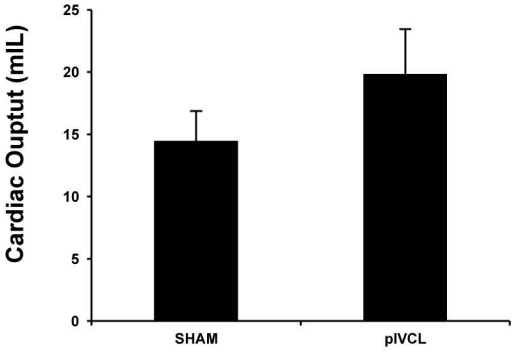

Supplement Figure 3

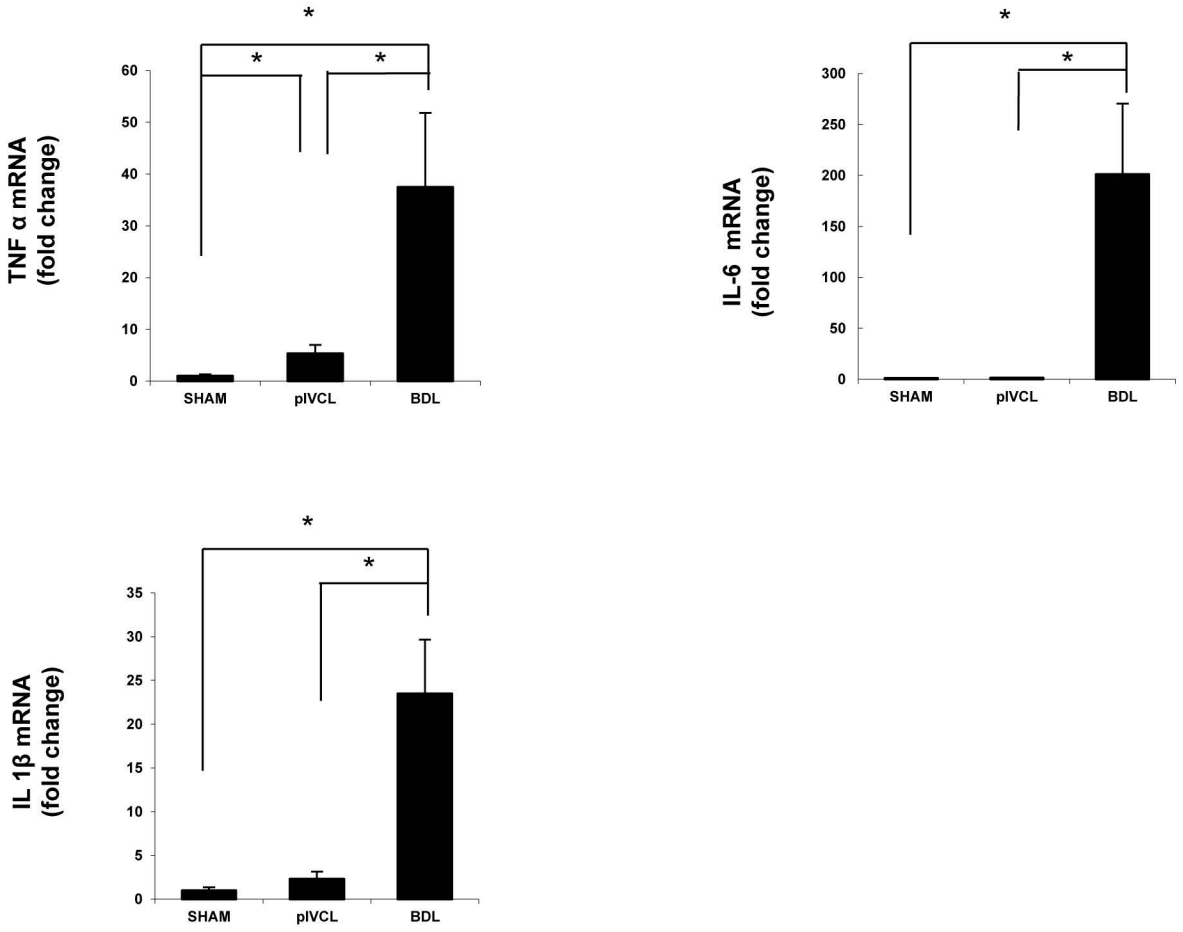

Supplement Figure 4

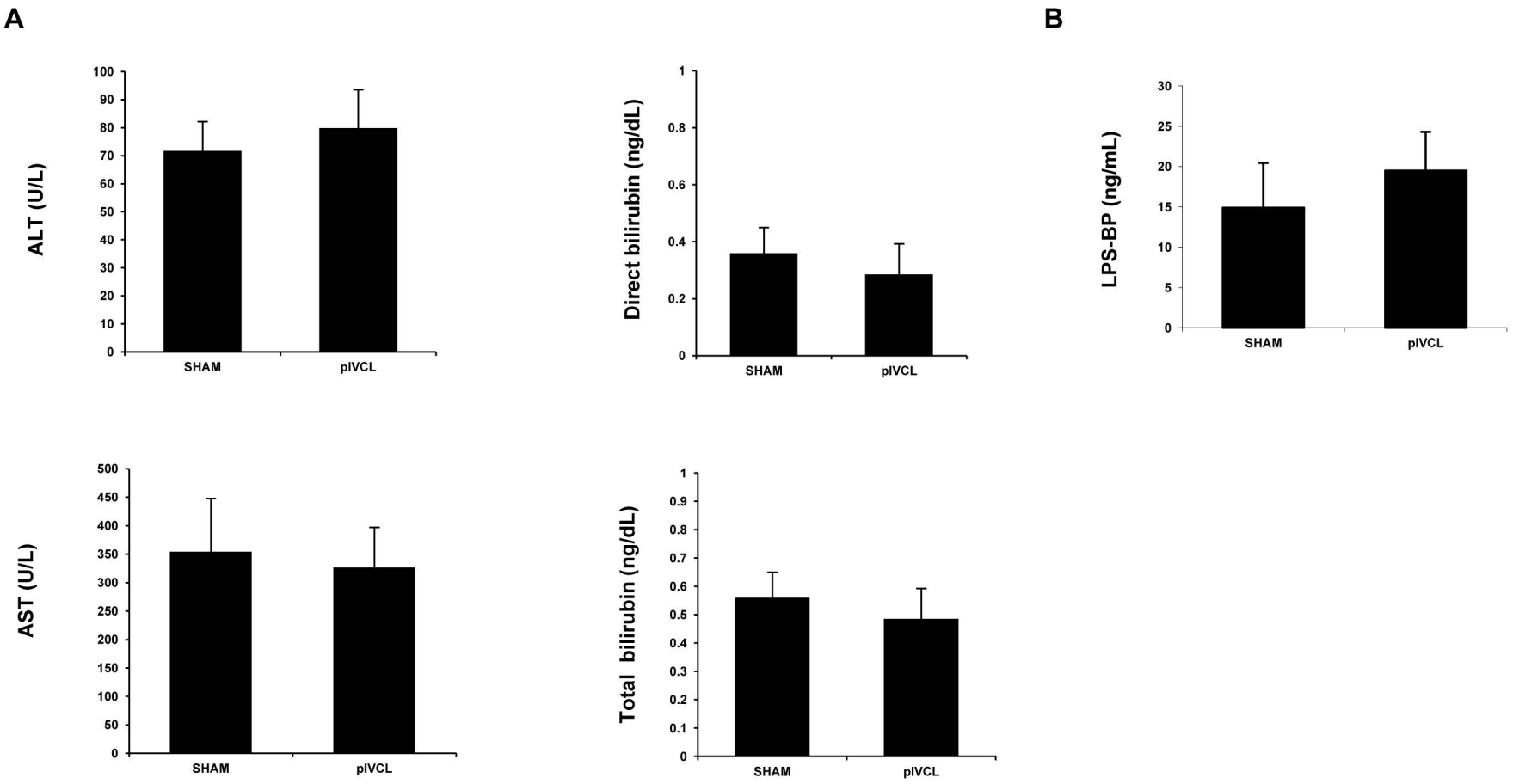

Supplement Figure 5

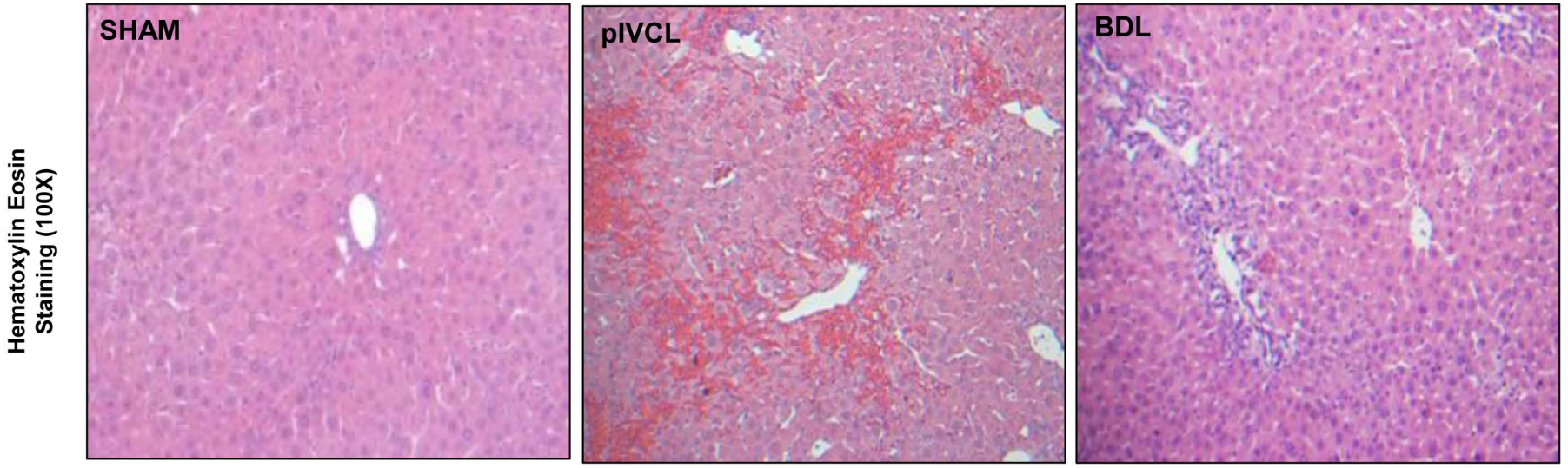

Supplement Figure 6

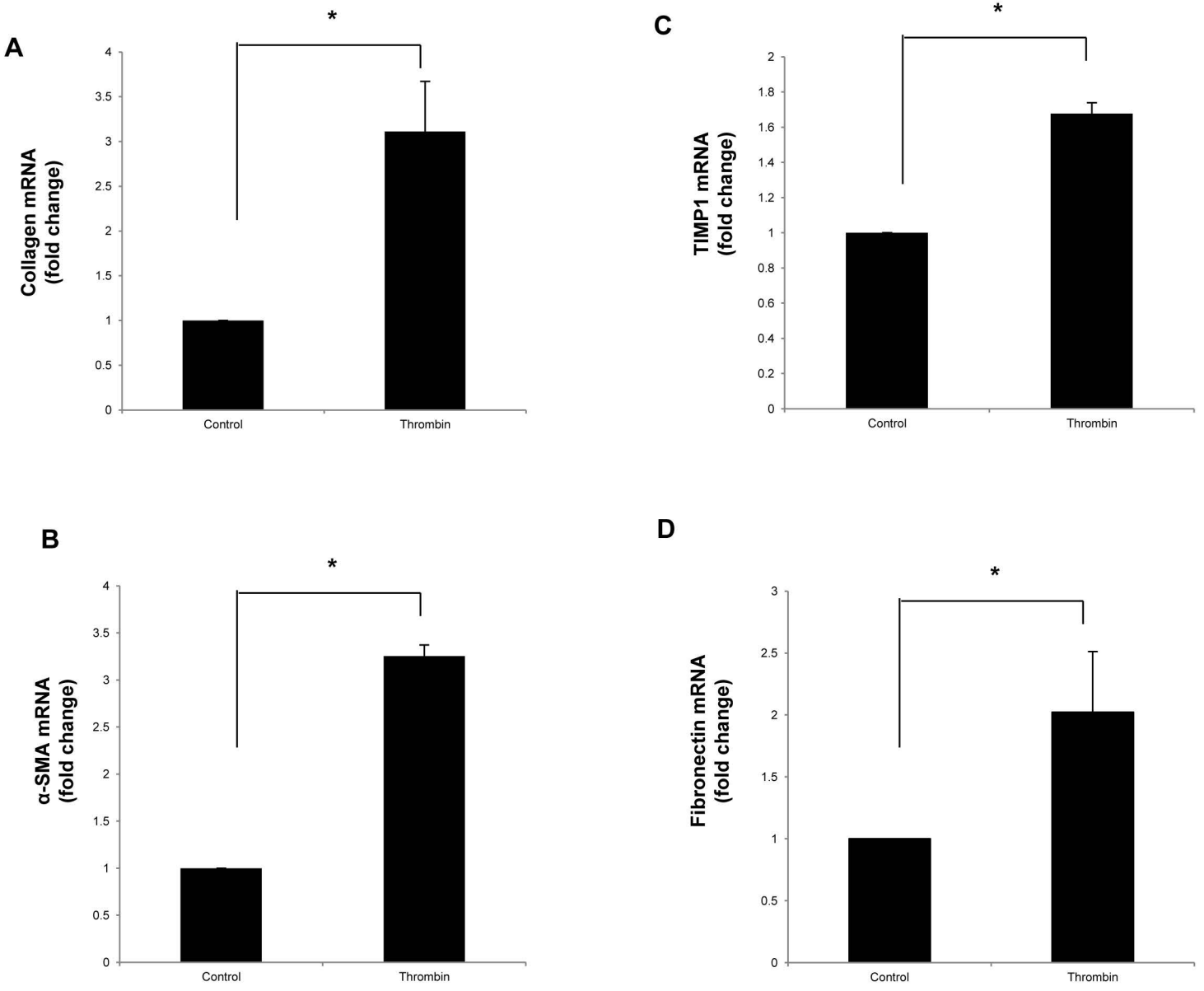

Supplement Figure 7

A

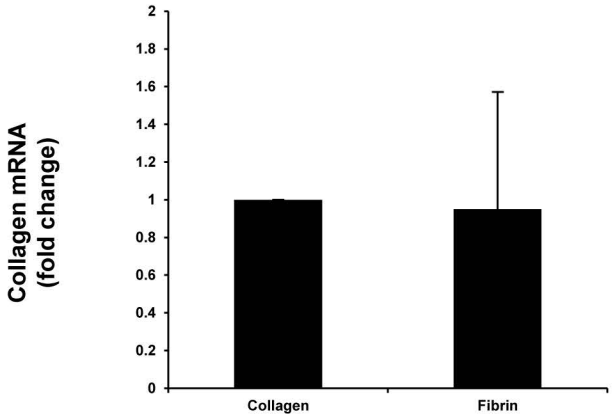

C

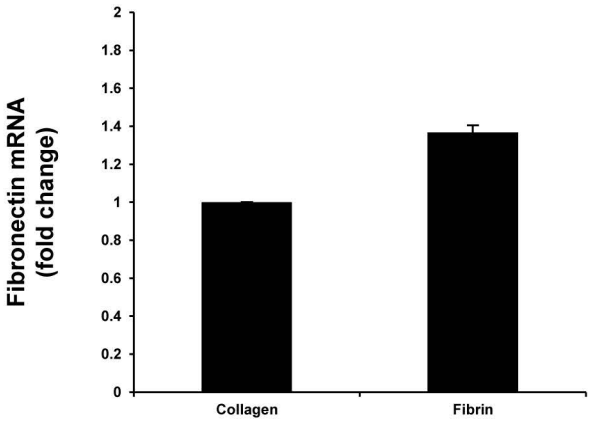

B

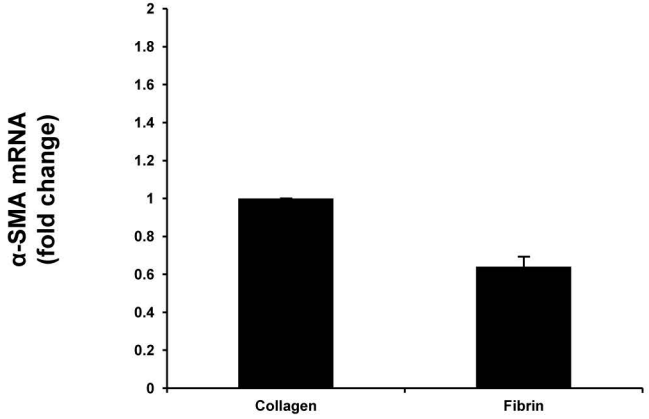

Supplement Table 1

Age	Gender	Sample	Fibrosis Stage (Metavir Score)	Primary Etiology
42	M	Transcutaneous Biopsy	Stage 4 (Cirrhosis)	Severe tricuspid regurgitation (TR)
76	M	Wedge Biopsy	Stage 1	Chronic left ventricular systolic heart failure
57	M	Liver explant	Stage 4 (Cirrhosis)	Severe left ventricular diastolic heart failure
29	F	Liver explant	Stage 4 (Cirrhosis)	Restrictive cardiomyopathy with severe TR
76	M	Wedge Biopsy	Stage 3	Chronic left ventricular systolic heart failure
51	F	Wedge Biopsy	Stage 1	Constrictive pericarditis
76	M	Wedge Biopsy	Stage 2-3	Restricitive cardiomyopathy with severe TR
53	F	Liver explant	Stage 4 (Cirrhosis)	Restricitive cardiomyopathy with severe TR
60	F	Liver explant	Stage 4 (Cirrhosis)	Chronic biventricular heart failure with severe TR
66	M	Liver explant	Stage 4 (Cirrhosis)	Chronic biventricular heart failure with severe TR
46	M	Liver explant	Stage 4 (Cirrhosis)	Chronic biventricular heart failure secondary to non-compaction cardiomyopathy
30	F	Liver explant	Stage 4 (Cirrhosis)	Restricitive cardiomyopathy with severe TR
62	M	Liver explant	Stage 4 (Cirrhosis)	Severe left ventricular diastolic heart failure
41	F	Liver explant	Stage 4 (Cirrhosis)	Restrictive cardiomyopathy with severe TR

Supplement Table 2

Age	Gender	Sample	Fontan procedure (age)	Fibrosis Stage (Metavir Score)
19	F	Transcutaneous Biopsy	4	Stage 2
26	M	Transcutaneous Biopsy	9	Stage 1
23	F	Transcutaneous Biopsy	2	Stage 2
46	M	Transcutaneous Biopsy	26	Stage 3-4 (Cirrhosis)
24	M	Transcutaneous Biopsy	9	Stage 3
33	F	Transcutaneous Biopsy	5	Stage 3
51	F	Transcutaneous Biopsy	25	Stage 3
21	F	Transcutaneous Biopsy	6	Stage 3
30	M	Transcutaneous Biopsy	4	Stage 2
29	M	Transcutaneous Biopsy	9	Stage 3
29	F	Transcutaneous Biopsy	11	Stage 4 (Cirrhosis)
34	F	Transcutaneous Biopsy	21	Stage 3

Supplement Table 3

Mouse		Sequence
α-SMA	Sense	AAACAGGAATACGACGAAG
	Antisense	CAGGAATGATTTGGAAAGGA
B-Actin	Sense	AGAGGGAAATCGTGCGTAC
	Antisense	CAATAGTGATGACCTGGCCGT
Fibronectin	Sense	GTGGCTGCCTTCAACTTCTC
	Antisense	GTGGGTTGCAAACCTTCAAT
Procollagen1-α1	Sense	GAGCGGAGAGTACTGGATCG
	Antisense	GCTTCTTTTCCTTGGGGTTC
TIMP-1	Sense	CCTTGCAAACTGGAGAGTGACA
	Antisense	AAGCAAAGTGACGGCTCTGGT

Human		Sequence
α-SMA	Sense	GGAGATCACGGCCCTAGCAC
	Antisense	AGGCCCGGCTTCATCGTAT
Fibronectin	Sense	GATAAATCAACAGTGGGAGC
	Antisense	CCCAGATCATGGAGTCTTTA
GAPDH	Sense	CTCTGCTCCTCCTGTTCGAC
	Antisense	TTAAAAGCAGCCCTGGTGAC
Procollagen1-α1	Sense	TGTGAGGCCACGCATGAG
	Antisense	CAGATCACGTCATCGCACAA
TIMP-1	Sense	GCTTCTGGCATCCTGTTGTT
	Antisense	TTGACTTCTGGTGTCCCCAC